

Helium stratification in HD 145792: a new He strong star^{*}

G. Catanzaro[†]

INAF - Osservatorio Astrofisico di Catania, Via S. Sofia 78, 95123 Catania, Italy

Accepted 2007 November 27. Received 2007 November 14; in original form 2007 October 16

ABSTRACT

In this paper we report on the real nature of the star HD 145792, classified as He weak in “*The General Catalogue of Ap and Am stars*”. By means of FEROS@ESO1.52m high resolution spectroscopic data, we refined the atmospheric parameters of the star, obtaining: $T_{\text{eff}} = 14400 \pm 400$ K, $\log g = 4.06 \pm 0.08$ and $\xi = 0^{+0.6}$ km s⁻¹. These values resulted always lower than those derived by different authors with pure photometric approaches.

Using our values we undertook an abundance analysis with the aim to derive, for the first time, the chemical pattern of the star’s atmosphere. For metals a pure LTE synthesis (ATLAS9 and SYNTHE) has been used, while for helium a hybrid approach has been preferred (ATLAS9 and SYNSPEC). The principal result of our study is that HD 145792 belongs to He strong class contrary to the previous classification. Moreover, helium seems to be vertically stratified in the atmosphere, decreasing toward deepest layers.

For what that concerns metals abundances, we found the following: overabundance of oxygen, neon, silicon, phosphorus, sulfur and calcium; carbon, nitrogen, magnesium, aluminum, titanium, chromium and nickel are normal, being the discrepancies from the solar values within the experimental errors; iron resulted to be slightly underabundant.

Key words: stars: chemically peculiar – stars: individual: HD 145792 – stars: abundances

1 INTRODUCTION

HD 145792 (=HR 6042 =V 1051 Sco) is a chemically peculiar star belonging to the Sco-Cen OB association (Morris (1961); Eggen (1998)) and classified as Helium weak star in the *General Catalogue of Ap and Am stars* by Renson et al. (1991). Hipparcos photometry has been analyzed by Paunzen & Maitzen (1998), they discovered light variability with a period of 0.84780 days. A few magnetic field measurements are present in the catalogue by Bychkov et al. (2003) with an average value of $H_{\text{eff}} = 285 \pm 190$ gauss.

Regarding atmospheric parameters, there are in the literature several inconsistent determinations of T_{eff} and $\log g$. For instance, Nissen (1974) found $T_{\text{eff}} = 16000$ K and $\log g = 4.34$, de Geus et al. (1989) found $T_{\text{eff}} = 15135$ K and $\log g = 4.38$ and Gulati et al. (1989) found effective temperatures ranging between 18450 K and 18920 K. All these studies are based on photometric approach. No previous abundances determination have been reported in the literature.

The principal aim of this study was to determine for the

first time the chemical abundances in the HD 145792’s atmosphere, with particular attention to helium behavior. With this goal in mind, we obtained high resolution spectrum of the star with FEROS@ESO1.52 m telescope. Atmospheric parameters like T_{eff} , $\log g$ and microturbulence have been derived by us with spectroscopic methods. In the following sections we present our results, giving particular emphasis to the actual peculiarity of the star: according to our results HD 145792 is a Helium strong star contrarily to the previous classification reported in Renson et al. (1991).

2 OBSERVATION AND DATA REDUCTION

A spectrum of HD 145792 in the 3600 - 9200 Å spectral range was obtained with the FEROS spectrograph on August 30, 2002 (HJD = 2 452 516.509) at the ESO 1.52 m telescope at La Silla Observatory, Chile. The spectral resolution was $R = 48000$.

The stellar spectrum, wavelength calibrated and normalized to the continuum, was obtained using standard data reduction procedures for spectroscopic observations within the NOAO/IRAF package. The resulting signal-to-noise ratio was ≈ 200 .

^{*} Based on observations collected at European Southern Observatory (ESO), La Silla, Chile, proposal ID 69.D-0537

[†] E-mail: Giovanni.Catanzaro@oact.inaf.it

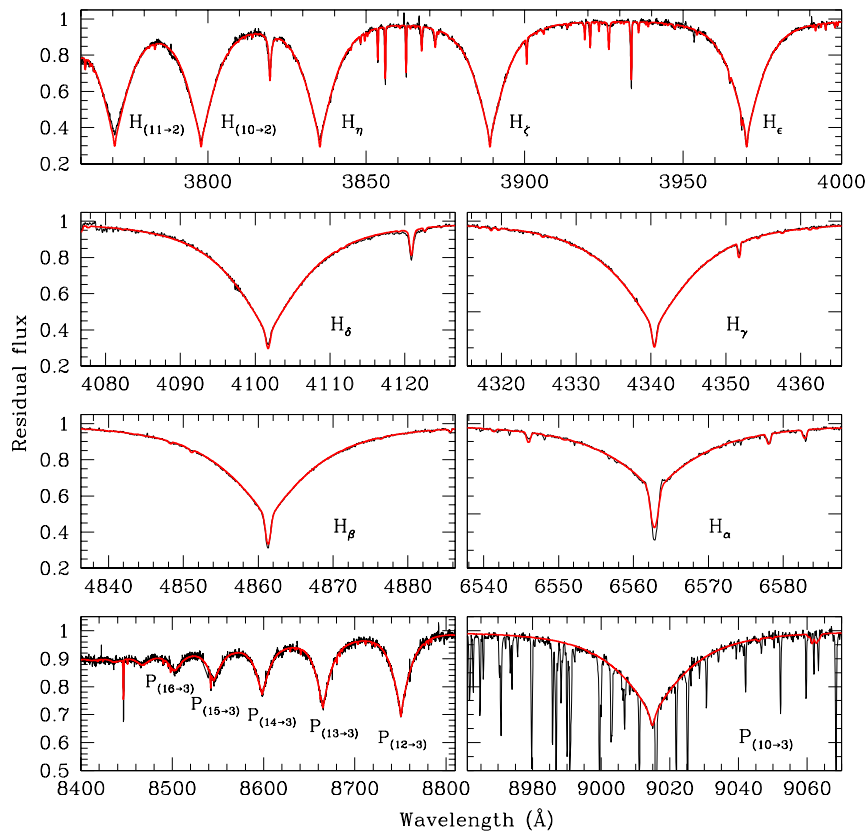


Figure 1. Comparison between the observed and computed hydrogen line profiles. From top to bottom: Balmer series from $H_{(n=11 \rightarrow 2)}$ to H_{α} and Paschen series from $P_{(n=17 \rightarrow 3)}$ to $P_{(n=10 \rightarrow 3)}$. The readers should note the strong telluric lines contamination around this line.

3 ATMOSPHERIC PARAMETERS

The approach we used in this paper was to minimize the difference between observed and synthetic H_{δ} , H_{γ} and H_{β} profiles. As goodness-of-fit test we used the parameter:

$$\chi^2 = \frac{1}{N} \sum \left(\frac{I_{\text{obs}} - I_{\text{th}}}{\delta I_{\text{obs}}} \right)^2$$

where N is the total number of points, I_{obs} and I_{th} are the intensities of the observed and computed profiles, respectively, and δI_{obs} is the photon noise. The synthetic spectra were generated in three steps: first, we computed the stellar atmosphere model by using the ATLAS9 code (Kurucz 1993) then, the stellar spectrum was synthesized using SYNTHÉ (Kurucz & Avrett 1981) and finally, the instrumental and rotational convolutions were applied. The ATLAS9 code includes the metal opacity by means of distribution functions (ODF) that are tabulated for multiples of the solar metallicity and for various microturbulence velocities.

Leone & Manfré (1997) determined T_{eff} , $\log g$, microturbulence velocity and abundances, minimizing χ^2 adopting an iterative procedure, but for H_{β} alone. Later, Catanzaro et al. (2004) extended this method using H_{δ} and H_{γ} as T_{eff} and $\log g$ indicators for non-solar composition atmospheres. In this study we extend the previous method to three Balmer lines: H_{δ} , H_{γ} and H_{β} . The intersection of the

three χ^2 iso-surfaces is expected to improve the final solution. Besides H_{α} is present in our spectral range, we did not use it principally for two reasons: *a)* it is located too close to the edge of the echelle order to be correctly normalized and *b)* for the intrinsic difficulties in modeling the line core with pure LTE approach.

To decrease the number of parameters, first of all we computed the $v_e \sin i$ of our star. To derive the rotational velocity, we used SYNTHÉ to reproduce the profile of $\text{MgII } \lambda 4481 \text{ \AA}$ line. Contrary to the value of 30 km s^{-1} reported by Abt et al. (2002), our best match with the observations was achieved convolving the computed profiles with a stellar rotational profile having $v_e \sin i = 18 \text{ km s}^{-1}$. As a by-product of this calculation we derived also its radial velocity: $RV = -4.34 \pm 0.43 \text{ km s}^{-1}$.

Then, to determine stellar parameters as consistent as possible with the actual structure of the atmosphere, we have reproduced the Balmer lines by the following iterative procedure:

- *a)* as starting values of T_{eff} and $\log g$ we have determined the effective temperature and gravity from Strömgren photometry according to the grid of Moon & Dworetzky (1985). The photometric colors have been de-reddened with the Moon (1985) algorithm. The source of the Strömgren photometric data was Hauck & Mermilliod (1998). Re-

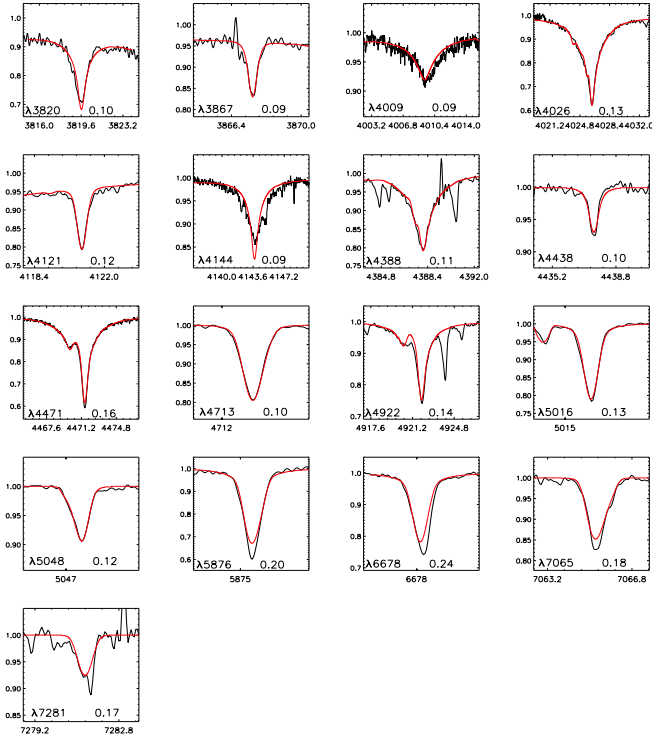


Figure 2. Comparison between observed and synthetic He I lines profiles. Due to the contamination of telluric lines the fits are not satisfactory for the last four lines. In the other cases only helium lines have been considered, that is the reason of absence of metallic lines. In each box we reported also the theoretical wavelength and the inferred abundance expressed as $n(\text{He})/n(\text{H})$.

sults of our calculations are: $T_{\text{eff}} = 15320 \pm 50$ K and $\log g = 4.27 \pm 0.04$;

- b) determination of T_{eff} and $\log g$ of the ATLAS9 atmosphere model whose H_δ , H_γ and H_β profiles, computed with SYNTHE, match the observations. The model has been computed using the opacity scale and abundances of the Sun;

- c) helium and metals abundances are derived and the microturbulent velocity determined independently from two sets of 10 SiII and 15 FeII lines¹ by requiring that the derived abundances do not depend on the measured equivalent widths;

- d) thus, we repeated the calculations described in step b) with the correct helium abundance, solar metallicity and ξ . For model calculations, we used a step of 50 K for T_{eff} and 0.01 dex for $\log g$.

The best fit was obtained for the model computed with the ODF for $[M/H]=0.0$, solar helium and:

$$\begin{aligned} T_{\text{eff}} &= 14400 \pm 400 \text{ K} \\ \log g &= 4.06 \pm 0.08 \\ \xi &= 0^{+0.6} \text{ km s}^{-1} \end{aligned}$$

Errors on T_{eff} and $\log g$ have been estimated within 1σ

¹ For the purpose of ξ determination we used all the lines with $\text{EW} > 10 \text{ m}\text{\AA}$

Table 1. Summary of the inferred abundances for each neutral helium lines detected in our spectrum. The three red lines without errors are those strongly contaminated by telluric contributions.

λ (Å)	$n(\text{He})/n(\text{H})$
3820.600	0.10 ± 0.01
3867.483	0.09 ± 0.02
4009.257	0.09 ± 0.02
4026.210	0.13 ± 0.03
4120.811	0.12 ± 0.03
4143.759	0.09 ± 0.01
4387.929	0.11 ± 0.02
4437.500	0.10 ± 0.02
4471.498	0.16 ± 0.03
4713.139	0.10 ± 0.03
4921.931	0.14 ± 0.03
5015.678	0.13 ± 0.02
5047.738	0.12 ± 0.03
5875.614	0.20
6678.152	0.24
7065.119	0.18
7281.349	0.17 ± 0.05

level of confidence, as the variation in the parameters which increases the χ^2 of a unit (Lampton et al. 1976).

The synthetic Balmer lines compared with the observed ones are showed in Fig. 1. With the atmospheric parameters found as described before, we attempted also in modeling the other hydrogen lines present in our spectral range, in particular from H_ϵ to the limit of the Balmer series (top panel of Fig. 1), H_α and the Paschen series from its limit at λ 8400 Å to the $P_{(n=10 \rightarrow 3)}$ at λ 9012 Å (bottom panels of Fig. 1). The good modeling of Paschen series with LTE synthesis, should not be a surprise as shown by Przybilla & Butler (2004).

4 ABUNDANCE ANALYSIS

Below we describe and comment on the abundance analysis for helium and metals in turn:

4.1 Helium

Neutral helium lines in a normal star with $T_{\text{eff}} \approx 13000$ are usually strong, even if the maximum strength is reached for the spectral type B2. To investigate the helium abundance we attempted to reproduce, by spectral synthesis, all the lines profiles observed in our spectrum.

Non-LTE effects play an important role in the formation of helium line, as known since the pioneering work by Auer & Mihalas (1972). Thus, because of the importance of NLTE effects, the synthetic helium lines were computed with the version 43 of the program SYNSPEC (Hubeny & Lanz 2000). This program reads the same input model atmosphere previously computed using ATLAS9 and solves the radiative transfer equation, wavelength by wavelength in a specified spectral range. SYNSPEC also reads the same Kurucz list of lines we used for the metal abundances. SYNSPEC allows one to compute the line profiles considering an approximate NLTE treatment even for LTE models. This is done

by means of the second-order escape probability theory (for details see the paper by Hubeny et al. (1986)). Moreover, the helium atom is considered explicitly and 14 levels of HeI are taken into account. For HeI $\lambda\lambda 4471$ Å detailed line broadening tables are taken from Barnard et al. (1974), for $\lambda\lambda 4026$, 4387 and 4922 Å from Shamey (1969) and for the other lines from Dimitrijevic & Sahal-Brechot (1984). Results of our modeling are displayed in Fig. 2, while inferred abundances with their errors have been reported in Tab. 1. These errors have been derived translating errors on atmospheric parameters into abundances uncertainties. Because of the presence of telluric lines contamination the fit of the lines: HeI $\lambda\lambda 5875$, 6678 and 7065 Å, is not satisfactory and the derived abundances have to be considered as low limits.

The first important result of this analysis is that helium is not underabundant, then HD 145792 could be ruled out from the He weak sub-class.

According to the calculations by Vauclair et al. (1991), helium is stratified in the atmospheres of magnetic CP stars: helium abundance increases with optical depth, reaches a maximum and then decreases. The position of the helium abundance maximum depends essentially on effective temperature, mass loss and diffusion strength. Vauclair's calculations have been verified for He strong stars by Leone & Lanzafame (1997) and Leone (1998). These authors performed spectroscopic observations in a sample of helium strong stars obtaining that helium abundance decrease going down through the atmospheres.

In order to search for helium stratification in HD 145792, we computed the contribution functions for the line cores of all helium lines reported in Fig. 2, calculations have been performed using the code XLINOP (Kurucz & Avrett 1981). In the upper panel of Fig. 3 we reported our abundances as a function of optical depth. We observed a constant and almost solar helium abundance ($n(\text{He})/n(\text{H}) \approx 0.1$) in the range of optical depths between 0.2 and -0.5, then helium seems to increase its abundance (up to $n(\text{He})/n(\text{H}) \approx 0.15$) going toward external layers. From this conclusion, we have excluded the three lines for which the strong telluric contamination did not allow us a good fit. Actually, if their contribute should be considered, helium abundance will increase up to $n(\text{He})/n(\text{H}) \approx 0.25$. In this case the effects of the change of the mean molecular weight in the atmospheric structure should be included.

Another important mark of the presence of stratification in the impossibility to reproduce the profile of a strong line with one abundance only. If we look at the $\lambda 4026$ Å we note that while the core is well reproduced the red wing is not. In particular the helium line at $\lambda 4023.973$ Å computed with the same abundance is stronger than that observed. This could be interpreted as another evidence in favor of stratification hypothesis.

4.2 Metals

To derive the metals abundances we identified all the unblended lines in the observed spectrum of HD 145792 using SYNTHE. The atomic parameters adopted in our analysis are from Kurucz & Bell (1995) line lists and subsequent update by Castelli & Hubrig (2004). In practice we divided all the spectrum in sub-intervals ≈ 100 Å wide and for each interval we performed a synthesis analysis. The final adopted

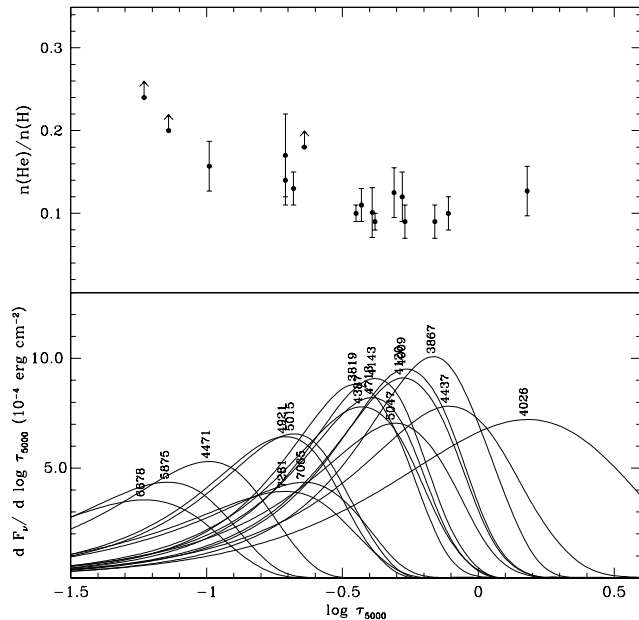


Figure 3. Helium stratification measured in HD 145792. The bottom panel shows the contribution functions computed for the lines core.

abundances are the weighted averages of these values and they are expressed in the usual form $\log N_{el}/N_{Tot}$.

Derived abundances are reported in Tab. 2 with their errors, in the same table for the sake of comparison we reported also the Sun abundances taken from Asplund et al. (2005). Errors on abundances have been estimated as the following: for all the elements for which we observed more than 5 spectral lines, we simply calculated the standard deviation; for the other cases we translated the errors on T_{eff} and $\log g$ in abundances uncertainties. The chemical pattern of HD 145792 is shown in Fig. 4. The principal result is an evident overabundance of neon with respect the solar case, a slight overabundance of oxygen, silicon, phosphorus, sulfur and calcium, iron appears to be slightly under the solar value and other elements are normal, being their discrepancies from the solar values within the experimental errors.

5 CONCLUSION

In this paper we report on the first abundances analysis ever presented in the literature on the star HD 145792. Principal results of our paper can be summarized in this two important points:

- the object resulted to be a He strong star, contrarily to the classification reported in Renson et al. (1991). The erroneous classification could be linked to effective temperatures and gravities reported in the literature that, as we discussed in Sect. 3, are always greater than ours ($T_{\text{eff}} = 14400 \pm 400$ K and $\log g = 4.06 \pm 0.08$).
- helium seems to be not homogeneously distributed along the atmosphere. It shows approximatively a constant and almost solar abundance from the inner layers up to

Table 2. Summary of the inferred abundances in the atmosphere of HD 145792. In the second column we reported the number of spectral lines used for the abundance determination. For comparison we reported the relative abundance in the solar photosphere (Asplund et al. 2005).

El	N	$\log N_{el}/N_{Tot}$	
		HD 145792	Sun
C	5	-3.57 ± 0.10	-3.64 ± 0.05
N	5	-4.15 ± 0.10	-4.25 ± 0.06
O	15	-3.16 ± 0.06	-3.37 ± 0.05
Ne	17	-3.66 ± 0.04	-4.19 ± 0.06
Mg	7	-4.56 ± 0.16	-4.50 ± 0.09
Al	9	-5.67 ± 0.05	-5.66 ± 0.06
Si	19	-4.38 ± 0.10	-4.52 ± 0.04
P	2	-6.45 ± 0.08	-6.67 ± 0.04
S	32	-4.70 ± 0.11	-4.89 ± 0.05
Ca	3	-5.44 ± 0.09	-5.72 ± 0.04
Ti	2	-7.05 ± 0.10	-7.13 ± 0.06
Cr	3	-6.50 ± 0.08	-6.39 ± 0.10
Fe	67	-4.74 ± 0.07	-4.58 ± 0.05
Ni	1	-5.85 ± 0.10	-5.80 ± 0.04

$\log \tau_{5000} = -0.5$ and a moderate increase toward the outer atmospheric layers (see Fig. 3)

For what that concern the chemical pattern of metals, we found, with respect the solar case, a strong overabundance of neon; a slight overabundance of oxygen, silicon, phosphorus, sulfur and calcium; iron appears to be slightly underabundant; the others elements are normal.

ACKNOWLEDGMENTS

This research has made use of the SIMBAD database, operated at CDS, Strasbourg, France

REFERENCES

- Asplund M., Grevesse N., Sauval A. J., The solar Chemical Composition. In: Cosmic Abundances as Record of Stellar Evolution, Barnes T. G., Bash F. M. (eds.), ASP Conf. Series, Vol. 336, 2005
- Auer L. H., Mihalas D., 1972, ApJS, 24, 193
- Abt H. A., Levato H., Grosso M., 2002, ApJ, 573, 359
- Barnard A. J., Cooper J., Smith E. W., 1974, JQRST, 14, 1025
- Bychkov V.D., Bychkova L.V., Madej J., 2003, A&A, 407, 631
- Castelli F., Hubrig S., 2004, A&A, 425, 263
- Catanzaro G., Leone F., Dall T. H., 2004, A&A, 425, 641
- Dimitrijevic, M. S., Sahal-Brechot, S., 1984, JQRST, 31, 301
- Eggen O. J., 1998, AJ, 116, 1314
- de Geus E. J., de Zeeuw P. T., Lub J., 1989, A&A, 216, 44
- Gulati R. K., Malagnini M. L., Morossi C., 1989, A&AS, 80, 73
- Hauck B., Mermilliod M., 1998, A&AS, 129, 431
- Hubeny I., Lanz T., 2000, SYNSPEC - A user's guide

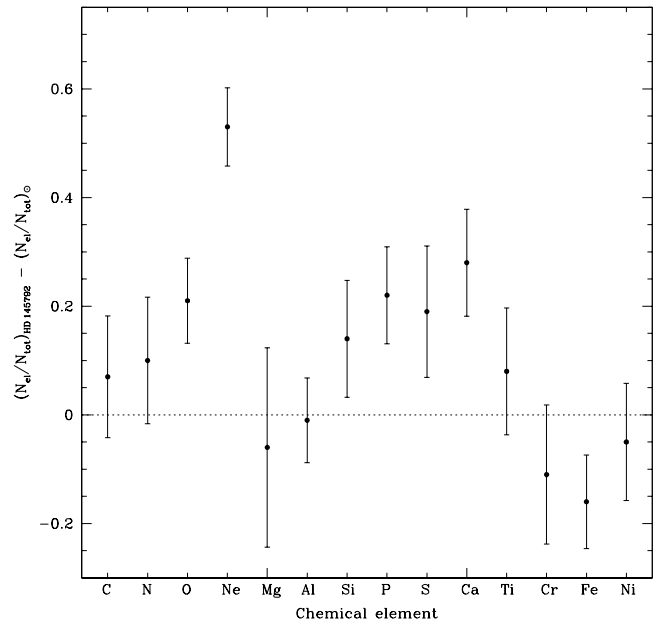


Figure 4. Abundance pattern computed for all metals detected in our spectrum.

- Hubeny I., Harmanec P., Stefl S., 1986, Bull. Astron. Inst, Czechoslovakia, 37, 370
- Kurucz R. L., Bell B., 1995, Kurucz CD-ROM No. 23. Cambridge, Mass.: Smithsonian Astrophysical Observatory.
- Kurucz R.L., 1993, A new opacity-sampling model atmosphere program for arbitrary abundances. In: Peculiar versus normal phenomena in A-type and related stars, IAU Colloquium 138, M.M. Dworetsky, F. Castelli, R. Faragiana (eds.), A.S.P Conferences Series Vol. 44, p.87
- Kurucz R.L., Avrett E.H., 1981, SAO Special Rep. 391
- Lampton M., Margon B., Bowyer S., 1976, ApJ, 208, 177
- Leone F., 1998, Contrib. Astron. Obs. Skalnaté Pleso, 27, 285
- Leone F., Manfré M., 1997, A&A, 320, 257
- Leone F., Lanzafame A. C., 1997, A&A, 320, 893
- Moon T. T., 1985, Comm. from the Univ. of London Obs., 78
- Moon T. T., Dworetsky M. M., 1985, MNRAS, 217, 305
- Morris P. M., 1961, MNRAS, 122, 325
- Nissen P. E., 1974, A&A, 36, 57
- Paunzen E., Maitzen H. M., 1998, A&AS, 133, 1
- Przybilla N., Butler K., 2004, ApJ, 609, 1181
- Renson P., Gerbaldi M., Catalano F.A., 1991, A&AS 89, 429
- Shamey P., 1969, PhD thesis, University of Colorado
- Vauclair S., Dolez N., Gough D. O., 1991, A&A, 252, 618